



Parameter Calibration in Global Land Carbon Models Using Surrogate-based Optimization

Haoyu Xu¹, Tao Zhang^{1,2}, Yiqi Luo^{2,3}, Wei Xue^{1,2}, Xin Huang^{1,2}

¹Department of Computer Science and Technology, Tsinghua University, Beijing 100084

5 ²Department of Earth System Science, Ministry of Education Key Laboratory for Earth System Modelling, Tsinghua University, Beijing 100084

³Department of Microbiology and Plant Biology, University of Oklahoma, Norman, Oklahoma, USA

Correspondence to: Wei Xue (xuewei@tsinghua.edu.cn)

Abstract. Soil organic carbon (SOC) has a significant effect on the carbon emission and climate change. However, current
10 SOC prediction accuracy of most models is very low. Most evaluation studies indicate that the prediction error mainly comes
from parameter uncertainties, which can be obviously improved by parameter calibration. Data assimilation technique has
been successfully employed for parameter calibration of SOC models. However, data assimilation algorithms such as Bayesian
Markov Chain Monte Carlo (MCMC) generally require a large amount of computation cost and are not appropriate for complex
15 global land models. This study proposes a new parameter calibration method based on surrogate optimization techniques for
improving the prediction of SOC. Experiments on three types of land carbon cycle models, including Community Land Model
with Carnegie-Ames-Stanford Approach biogeochemistry sub-model (CLM-CASA') and two microbial models show that
surrogate-based optimization method is more effective and efficient than MCMC on both accuracy and cost. The root mean
squared errors (RMSE) between predictions of different SOC models calibrated by surrogate-base optimization and
20 observations can be reduced up to 12% compared to the results by using Bayesian MCMC. Meanwhile, the corresponding
computation cost required is only one thousandth of that with Bayesian MCMC.

1 Introduction

Soil organic carbon (SOC) is the largest pool of global land carbon. The emission of CO₂, a famous greenhouse gas, from the
land ecosystems greatly depends on the amount of carbon stored in soils. Simultaneously, more emitted CO₂ increases the
climate warming (Houghton et al., 2001) and the climate warming intensifies soil carbon release, resulting in a positive
25 feedback cycle between carbon cycle and climate warming (Melillo et al., 2003; Friedingstein et al., 2006; Luo, 2007). In the
fifth Coupled Model Intercomparison Project (CMIP5), the outputs of 11 Earth system models (ESMs) show great uncertainty
in the SOC predictions and simulations. Despite the similarity in model structures, simulated soil carbon content varies six-
fold among the models with the simulations ranging from 510 to 3040 PgC (Todd-Brown et al., 2013). Only half of 11 model
outputs agree with the estimates of the Harmonized World Soil Database (HWSD) and even the highest correlation coefficients
30 between model output and observation is lower than 0.4 (Todd Brown et al., 2013; Luo et al., 2015).



Considering the high similarity in the carbon cycle component structures of the 11 ESMs, the differences of SOC simulations mainly comes from the parameterizations (Todd Brown et al., 2013), and thus the parameter calibration can improve the simulation of carbon cycle a lot (Luo et al., 2016). However, the parameter calibration with global data has not been widely applied owing to the expensive computational cost. The Bayesian Markov chain Monte Carlo (MCMC) algorithm has been used for parameter calibration of SOC simulation and microbial process successfully (Harauk et al., 2014, 2015). Bayesian MCMC usually requires a large number of simulations on building the accepted parameter chain; for instance, over 500,000 simulations are required when calibrating soil carbon parameters (Harauk et al. 2014, 2015). Even using the high performance computers to provide the computation power, some complex models like CLM require several hours or days for only one simulation. Comprehensively, Bayesian MCMC cannot be extended to expensive global land models such as the Community Land Model (CLM). More effective and efficient parameter calibration algorithms are intensively demanding.

Parameter calibration of SOC models can be formulated to optimization problems that aim to minimize a metric function value. The metric function evaluates the difference between model simulations and the corresponding observations and returns a single value to represent the model error. Global optimization algorithms are introduced to solve minimization of non-linear, non-convex and black-box problems (Hapuarachchi et al., 2001; MA H, et al., 2006; Rocha H, 2008). Unfortunately, the required simulation times of most global optimization are also very large.

To decrease the computational cost also the simulation times, we for the first time present the surrogate-based optimization method for improving the prediction of SOC. Surrogate models serve as computationally cheap approximations of the expensive simulation model (Booker et al., 1999), such as complex geoscientific models. During the optimization, surrogate model is used to carefully determine a new promising point in the parameter domain at which the computationally expensive simulation model needs be evaluated. Many unnecessary simulations with bad parameter values are avoided based on the prediction of the surrogate model. Surrogate-based optimization has been proved to find near-optimal parameters within only few hundred simulations (Aleman et al., 2009; Giunta et al., 1997; Regis, 2011; Simpson et al., 2001).

Quite a few studies about global and surrogate optimization focus on the benchmarks consisting of mathematical functions like COCO (Comparing Continuous Optimisers) benchmark (Hansen et al., 2010; Wang and Duan, 2014). The optimization of mathematical functions is extremely different from the parameter calibration of complex real-world models. Here for the first time, we tried to exploit state-of-the-art surrogate optimization method for the parameter calibration of three types of soil organic carbon (SOC) models and compared the performance of surrogate-based optimization to advanced global optimization algorithms and the data assimilation method. The evaluation and analysis based on three representative SOC models can be extended to other complex SOC models including CLM. On average, the RMSE of new calibrated SOC prediction is 0.68 kg/m^2 lower than that calibrated by Bayesian MCMC and the computation cost is only about 0.1% of Bayesian MCMC. This paper is organized as follows. Section 2 presents the structure and parameters of three representative SOC models. In Section 3, we briefly introduce the scheme and design of the surrogate-based optimizations. The parameter calibration results and the analysis of different parameter calibration algorithms are presented in Section 4. Section 5 analysis the calibrated results of the surrogate-based optimization. Finally, we draw conclusions in Section 6.



2 Global Land Carbon Models and Metrics

Earth system models (ESMs) are the fundamental tools for simulating climate impacts on carbon cycle at the global scale and their structures of land carbon cycle are almost the same. They define different carbon pools such as soil and litter pools. Carbon transfer among these pools by respiration (Todd Brown et al., 2013; Weng and Luo, 2011). In this study, we selected three types of SOC models. These models are summarized and extracted from global land models. They keep the key equations and structures of carbons transferring and thus they are representative. The first model is the soil carbon component of the Community Land Model coupled with Carnegie-Ames-Stanford Approach biogeochemistry submodel (CLM-CASA') (Oleson et al., 2004, 2008). The CLM is the land model for the Community Earth System Model (CESM), which is one of the most popular earth system models in the world. It is also a collaborative project between scientists in the Terrestrial Sciences Section (TSS) and the Climate and Global Dynamics Division (CGD) at the National Center for Atmospheric Research (NCAR) and the CESM Land Model Working Group. The other two SOC models are microbial models. These two models consider microbial biomass dynamics explicitly which most conventional SOC models like CLM-CASA' don't take into account. The calibrated microbial models explain more variability of the observed SOC (Hararuk, 2015). Considering the similarity in model structures, these three types of SOC models can represent the structures of the SOC components in most of current land models (Luo and Weng, 2011).

2.1 CLM-CASA' C-only Version Model

The CLM-CASA' includes biogeophysics and biogeochemistry submodels. Carbon transferring among various plants, litter, and soil pools are simulated in the biogeochemistry submodels (Parton et al., 1993). The influx into and efflux from each pool determines the carbon content of the pool. Carbon influx into the whole system is partitioned among three live biomass pools. Carbon efflux is heterotrophic respiration which is determined by decomposition rate of organic carbon in each pool. Heterotrophic respiration is also influenced by environmental conditions (especially, temperature and soil moisture), soil texture, and tissue lignin and tissue available nitrogen content.

The CLM-CASA' simulates soil carbon decomposition as a first-order decay process (Todd-Brown et al., 2013b). Based on theoretical analysis, carbon cycle of most ESMs can be summarized to some linear system differential equations (Luo and Weng, 2011; Xia et al., 2013) as

$$\frac{dX(t)}{dt} = A\xi(t)KX(t) + BU(t) \quad (1)$$

Where $X(t)$ is the carbon content of different pools; $\frac{dX(t)}{dt}$ is the change of the carbon content; A is a matrix of partitioning coefficients among different pools; $\xi(t)$ and K are both diagonal matrixes, representing environmental factors and baseline carbon exit rates, respectively; $U(t)$ is the carbon influx into the whole system and B represents the partitioning coefficients of the carbon influx. The steady solution of equation (1) is solved by Xia et al. (2012):

$$X_{ss} = -(A\bar{\xi}K)^{-1}\bar{B}\bar{U} \quad (2)$$



Where $\bar{\xi}$, \bar{B} , and \bar{U} are long-term averages of the environmental scalars, C partitioning among the three live pools, and NPP respectively. The structure details of CLM-CASA' C-only model are presented in Fig. 1a and parameters are described in Table 1. The steady state soil C generated by this C-only version agreed largely with that simulated by original CLM-CASA' model (Xia et al., 2012).

5 2.2 The Microbial Models

Microbial process has various kinds of effects on the land carbon cycle, such as the real priming effects and increasing temperatures caused by soil microbial biomass (Kuzyakov et al., 2000; Luo et al., 2001; Peng et al., 2009). However, most conventional SOC models including CLM-CASA' do not explicitly represent microbial processes. Considering the microbial processes, the SOC decomposition rate is controlled by extracellular enzyme concentrations, not simple decay constants in the CLM-CASA' and other traditional SOC models (Schimel and Weintraub, 2003). In this study, we focused on two enzyme driven decomposition models, one has two pools (Fig. 1b) introduced by German et al. (2012) and Hararuk et al. (2015), and the other has 4 pools (Fig. 1c) introduced by Allison et al. (2010). We call these two models 2-pool microbial model and 4-pool microbial model, respectively. The 2-pool microbial model is described as the following equations.

$$\frac{dMIC}{dt} = CUE \times V_{max} \times MIC \frac{SOC}{K_m + SOC} - r_d \times MIC \quad (3)$$

$$15 \quad \frac{dSOC}{dt} = Input_{soil} + r_d \times MIC - V_{max} \times MIC \frac{SOC}{K_m + SOC} \quad (4)$$

with

$$CUE = CUE_{slope} \times T_s - CUE_0 \quad (5)$$

$$V_{max} = V_{max_0} \times \exp\left(-\frac{E_a}{R \times (T_s + 273)}\right) \times \exp(-par_{clay} \times clay) \quad (6)$$

$$Km = Km_{slope} \times T_s + Km_0 \times \exp(par_{lig} \times lignin) \quad (7)$$

20 MIC represents the microbial biomass and SOC represents the soil organic carbon pool. $Input_{soil}$ is the carbon influx to soil. The others are parameters to be calibrated and listed in Table 2. The first eight parameters in Table 2 belong to the 2-pool microbial model.

The 4-pool microbial model from Allison et al. (2010) is described as:

$$\frac{dMIC}{dt} = V_{maxup} \times MIC \frac{DOC}{K_{mup} + DOC} \times CUE - r_d \times MIC - r_{EnzProd} \times MIC \quad (8)$$

$$25 \quad \frac{dDOC}{dt} = a_{lit-to-DOC} \times Input_{soil} + r_d \times MIC \times (1 - a_{MIC-to-SOC}) + V_{max} \times ENZ \frac{SOC}{K_m + SOC} + r_{EnzLoss} \times ENZ - V_{maxup} \times MIC \frac{DOC}{K_{mup} + DOC} \quad (9)$$



$$\frac{dSOC}{dt} = a_{lit-to-SOC} \times Input_{soil} + r_d \times MIC \times a_{MIC-to-SOC} - V_{max} \times ENZ \frac{SOC}{Km+SOC} \quad (10)$$

$$\frac{dENZ}{dt} = r_{EnzProd} \times MIC - r_{EnzLoss} \times ENZ \quad (11)$$

With

$$CUE = CUE_{slope} \times T_s - CUE_0 \quad (12)$$

$$5 \quad V_{maxup} = V_{maxup_0} \times \exp\left(-\frac{E_{aup}}{R \times (T_s + 273)}\right) \quad (13)$$

$$Kmup = Kmup_{slope} \times T_s + Kmup_0 \quad (14)$$

$$V_{max} = V_{max_0} \times \exp\left(-\frac{E_a}{R \times (T_s + 273)}\right) \times \exp(-par_{clay} \times clay) \quad (15)$$

$$Km = Km_{slope} \times T_s + Km_0 \times \exp(par_{lig} \times lignin) \quad (16)$$

Where *ENZ* and *DOC* are enzyme and dissolved organic carbon pools, respectively. Compared to the 2-pool version, the 4-pool microbial model has additional 7 parameters to calibrate. Total 15 parameters of the 4-pool microbial model are described in Table 2.

2.3 Data and Metrics

Microbial models and CLM-CASA' C-only models divide the world into 64*128 grid cells and output SOC quality of each grid (Fig. 2). The observation SOC data for parameter calibration comes from the International Geosphere Biosphere Programme – Data and Information System (IGBP-DIS) dataset (Global Soil Data Task Group, 2000). IGBP-DIS dataset includes a 1-km resolution global land carbon data set and the dataset has been widely used in many studies to evaluate and improve models (Zhou et al., 2009; Smith et al., 2013).

The goal of parameter calibration is to improve SOC predictions such that the model better fits the observations. Therefore, we use the root mean squared errors (RMSEs) between the model SOC predictions and the observations at all grid cells as the metric function. The metric function (RMSE) can be described as the following formula:

$$r = \sqrt{\frac{1}{N} \sum_{i=1}^N (X_i - O_i)^2} \quad (17)$$

Where *N* denotes the total number of grid cells, *X_i* and *O_i* are the SOC of model prediction and IGBP-DIS observation, respectively. To avoid overfitting and evaluate the calibrated parameters more fairly, we separate all grid cells into training set and validation set. The training set is used to guide the parameter calibration process and the validation set is used to evaluate



the calibrated results. Hararuk et al. also use this method when calibrating SOC parameters with the Bayesian MCMC approach (2014, 2015). The experiment results in Section 3 and 4 are refer to the validation set.

3 Surrogate-Based Optimization Algorithm Design

The scheme of the surrogate-based optimization (referred as SBO hereafter) is presented in Fig. 3. Firstly, initial sets of parameter values are generated using a sampling method. These points are then used as inputs to run the real simulation model. Secondly, a surrogate model is constructed by fitting the sampling points. The surrogate model serves as computationally cheap approximation of the expensive simulation model (Booker et al., 1999). Then in each iteration, new sample points are generated according to specific strategies. The strategy can make use of the information gained from the surrogate model. The new sample points and their simulation results are used to update the model at the same time. Finally, when some stop criteria (usually the maximum allowed number of simulations) are met, the algorithm return the optimized parameter values. During surrogate-based optimization process, new parameter points are generated based on the information of the surrogate model and most meaningless simulations with terrible parameter values are cancelled. As a result, the computationally expensive model is simulated at only a few selected promising parameter points and thus SBO can save much computation cost.

There are three critical steps while designing the surrogate-based optimization algorithms: the surrogate model, the initial sampling and the parameter point generation. There are various surrogate models such as multivariate adaptive regression splines (Friedman, 1991), polynomial regression models (Myers and Montgomery, 1995), radial basis functions (RBFs) (Gutmann, 2001; Müller et al., 2013; Powell, 1992; Regis and Shoemaker, 2007, 2009; Wild and Shoemaker, 2013), kriging (Davis and Ierapetritou, 2009; Forrester et al., 2008; Jones et al., 1998). Many machine learning regression models are also introduced like support vector regression (Zhang et al., 2009), artificial neural network (Behzadian et al., 2009) and random forest (Breiman, 2001). However, these machine learning regression models perform not so well as RBF and kriging models according to the evaluation on some cases (Wang et al., 2014). In this study, we use the RBF surrogate model because it has been proved to perform better than other surrogate model types (Müller and Shoemaker, 2014) and thus we call our method RBF-SBO later.

We use symmetric Latin hypercube sampling (LHS) at the initial sampling method for LHS ensures that the ensemble of random numbers is representative of the real variability whereas traditional random sampling is just an ensemble of random numbers without any guarantees.

The parameter point generation strategies are iterative algorithms that use data acquired from previous iterations to guide new parameter point generation. Most strategies convert the parameter point generation task to optimization problems using an evaluation criterion (Fig. 3). There are many different new parameter point generation strategies, including “Minimizing an Interpolating Surface (MIS)” (Jones, 2001) and “Maximizing Expected Improvement (MEI)” (Schonlau et al., 1997; Picheny et al., 2013). In MIS, the minimum of the surrogate model response surface is found and treated as the new parameter point to evaluate at the real simulation model and update the surrogate model. The disadvantage of MIS is that it does not take the



uncertainty of the surrogate model into account and puts too much emphasis on exploiting in a certain region and no emphasis on exploring uncertain points that have not been explored. As a result, MIS can be very efficient but easy to trap into local optimum. To eliminate the disadvantage of MIS, MEI introduces the “expected improvement” criterion. The expected improvement criterion estimates the uncertainty of the surrogate model and balance the exploration and exploitation. However, MEI can only be used for the kriging surrogate model as the calculation of the expected improvement requires the standard error at the parameter point and only the kriging (Gaussian Process) surrogate model can provide the standard error. In this study, we try to present hybrid evaluation criteria for choosing new parameter points in the “candidate point approach (CAND)” (Regis and Shoemaker, 2007). The criterion for exploitation is MIS and the criterion for exploration is the distance of the candidate point to the set of sampled parameter points from previous iterations. The previous sampled points represent the explored region and we can estimate the uncertainty with the distance to the explored region. A weighted sum of these two criteria is employed to determine the new parameter point during our surrogate-based optimization.

4 Parameter Calibration Experiments

4.1 Experiment Configuration

In this study, we select the Bayesian MCMC approach and four advanced global optimization algorithms to compare with our proposed surrogate-based optimization method. The three types of SOC models and metric function are introduced in Section 2. The target of parameter calibration is to find the parameters of the minimum metric function value (average RMSE). To ensure the stability of results, we repeat the parameter calibration process of each algorithm 50 times to evaluate the stability of algorithms. We compare the performance of algorithms from both the effectiveness and efficiency. The effectiveness means the accuracy of the calibrated results and the efficiency can be evaluated by the required simulation times.

4.2 Various Global Optimization Algorithms and the Bayesian MCMC Approach

The Bayesian MCMC approach and four advanced global optimization algorithms including Differential Evolution (DE), Particle Swarm Optimization (PSO), Shuffled Complex Evolution (SCE-UA) and Covariance Matrix Adaption Evolution Strategy (CMA-ES) are used to compare with our RBF surrogate-based optimization.

DE (Storn and Price, 1997) and PSO (Kennedy, 1995; Shi and Eberhart, 2009) are the outstanding representative algorithms of the evolution strategy and swarm intelligence, respectively. They both have the ability to quickly converge and outperform many versions of genetic algorithms and simulated annealing (Price and Storn, 2006; Shi and Eberhart, 2009). SCE-UA (is targeted for the parameter calibration of hydrologic models and has gained success in various hydrology models such as the TOPMODEL, the Xinanjiang watershed model and short-term load forecasting (Hapuarachchi et al., 2001; MAH, et al., 2006; Li G, et al., 2007). SCE-UA ensures the effectiveness and efficiency by combining the local (the simplex method) and global optimization methods. Despite the difference in detail, DE, PSO and SCE-UA all generate new parameter points according to some simple mathematical formula. In contrast to the three algorithms, CMA-ES (Hansen and Ostermeier, 2001; Hansen and



Kern, 2004) creates new parameter points based on a multivariate norm distribution. The dependencies between parameters are represented by the covariance matrix of the norm distribution. CMA-ES is proved to be the best global optimization algorithm on the BBOB-2009 comparison study (Hansen, 2009).

The Bayesian MCMC approach consists of two steps: the proposing step and the moving step. In the proposing step, the parameter covariance matrix is estimated from a parameter chain. A new parameter set is generated from the last accepted parameter set through a uniform proposal distribution when building the parameter chain (Xu et al., 2006). In the moving step, a probability of acceptance determined by prediction error is calculated (Marshall et al., 2004). The final calibrated parameter set is estimated by Maximum likelihood estimator (MLE) with the accepted parameter chain. Hararuk et al. (2014, 2015) applies the Bayesian MCMC approach to parameter calibration of the CLM-CASA' C-only model and microbial models. During experiments of Hararuk et al. (2014, 2015), the proposing step requires 50,000 simulations and the moving step requires 500,000 simulations for microbial models and 1,000,000 simulations for the CLM-CASA' model. The detail of the Bayesian MCMC approach calibration is presented in Table 3.

4.3 Results and Analysis

4.3.1 Effectiveness and Efficiency

Fig. 4 presents the calibrated RMSE of different algorithms we measure. For each of the global optimization algorithms and our SBO algorithm, we only perform 100 simulations for comparison. As the requirement of Bayesian MCMC algorithm, over 500000 simulations have conducted for this algorithm.

Obviously, the average RMSE of the RBF-SBO is the lowest (0.6 kg/m^2 better than the Bayesian MCMC algorithm) for two microbial models among all the tested algorithms (Fig. 4b, c). On the CLM-CASA' model, our RBF-SBO algorithm is still the best one compared to the global optimization algorithms. And the Bayesian MCMC approach gets a little better result (only about 0.02 kg/m^2) since it has a lot of more simulations and can exploit better results (Fig. 4a).

From the aspect of stability, the RBF-SBO also shows lower variation among the 50 repeating experiments compared with the global optimization algorithms on three types of models. For the same reason mentioned before, the Bayesian MCMC approach get lower variation than our RBF-SBO algorithm on two microbial models. For the most complex CLM-CASA' model, our RBF-SBO is still the promising one on stability. Among the global optimization algorithms, the CMA-ES shows very significant variance (Fig. 4b, c), indicating CMA-ES is unreliable when the number of simulations is 100. It is because the CMA-ES spends quite a few simulations on the exploration of the parameter domain and constructing the parameter covariance matrix and thus that CMA-ES shows high variance with fewer simulations. Therefore, our RBF surrogate-based optimization is the most effective and stable when the number of simulations is limited, which is extremely critical for those expensive models.

Fig. 5 shows the results in terms of average validation RMSE. The Bayesian MCMC is not shown for it requires at least 50000 simulations in the proposing step. The average validation RMSE of RBF-SBO is lower than other four global optimization



algorithms till 600 simulations on two microbial models and 200 simulations on the CLM-CASA' model, respectively. The number of simulation our RBF-SBO requires is fewer than other global optimization algorithms when being required to reach a target RMSE value or some accuracy range. Thus, our RBF surrogate optimization is also the most efficient algorithm which requires the minimum simulation times as well as computation cost.

- 5 Another observation is that the difference between our RBF-SBO and other global optimization algorithms decreases as the number of simulation increases (Fig. 5). Moreover, the CMA-ES outperforms the RBF-SBO while the number of simulation exceeds 200 on the CLM-CASA' model (Fig. 5a). As we know, the surrogate model is only the approximation of the real model and the accuracy is limited by many factors including the sample size, the nonlinearity and complexity of the real model. At the start of SBO, the approximate surrogate model can guide the algorithm to find a near-optimal solution and the accuracy of the surrogate model is also improved simultaneously. However, the accuracy of the surrogate model has limits and may not find the most accurate solutions.

4.3.2 Impact of the Model Complexity

- 15 Compared to the 2-pool and 4-pool microbial models, the CLM-CASA' model has 13 carbon pools and 20 parameters and thus that the CLM-CASA' model is significantly more complex than two microbial models. Despite the increasing complexity of the CLM-CASA' model, the SBO keeps ahead till 200 simulations (Fig. 5a). Moreover, the SBO is always the best parameter calibration method of the 2-pool and 4-pool microbial models before 600 simulations (Fig. 5b, c). Only one global optimization algorithm, CMA-ES, shows better performance than the SBO on the CLM-CASA' model after about 200 simulations. Considering the high variance of CMA-ES on two microbial models (Fig. 4b, c), the SBO is better and more reliable than the CMA-ES, on average.

20 4.3.3 Impact of Different Types of Surrogate Models

- We select the RBF as the surrogate model in the former experiments as the RBF is promising and the default choice in many specific surrogate-based optimization algorithms (Müller and Shoemaker, 2014). In this section, we also involve two other typical surrogate models, kriging and the multivariate adaptive regression splines (Mars). The Mars model is simple to understand and interpret and has almost no requirements for the samples. On the other hand, Mars is very quick to train and predict. The kriging, also Gaussian process regression, is a method of interpolation for which the interpolated values are modeled by a Gaussian process governed by prior covariance. Kriging gives the best linear unbiased prediction of the intermediate values under suitable assumptions on the priors.

- 25 Fig. 6 presents the results of kriging, Mars and RBF in terms of average validation RMSE. The performance of the three surrogate models are very similar and no one can dominate other two all the time. The three surrogate models all get success in the parameter calibration of the three types of SOC models and perform better than global optimization algorithms, indicating that our surrogate-based optimization is robust.



5 Analysis of Parameter Calibration Results

5.1 Analysis of CLM-CASA' Model

The steady global SOC simulations (Equation (2)) with the default and calibrated parameter values are presented in Fig. 7a and b, which we then compare to observed SOC pools provided by IGBP-DIS dataset. Obviously, the SOC simulation result after parameter calibration using the surrogate-based optimization matches observation better than SOC prediction by the default parameter values (Fig. 7c). Compared to SOC produced by CLM-CASA' with the default parameters, the size of SOC produced by the CLM-CASA' model with the calibrated parameters increases with decreased RMSE. After parameter calibration, SOC simulations are significantly improved almost all over the world, except some grid cells in the west of Canada and the east of Russia (Fig. 7a, b). As a result, the CLM-CASA' model with the default parameters explains 33% of variation in the observed soil C, whereas the CLM-CASA' model with the calibrated parameters explain 41% of variability in the observed soil C.

Fig. 8 presents the frequency distributions of the 20 calibrated parameters of MCMC. The blue line in Fig. 8 represents the calibrated parameters of the surrogate-based optimization. Sharp posterior distributions indicate that those are highly sensitive parameters, agreeing with the conclusions of Hararuk et al. (2014) and Post et al., (2008). The calibrated parameters of the surrogate-based optimization agree with the posterior distributions in most highly sensitive parameters such as temperature sensitivity of heterotrophic respiration (Q_{10}) and clay effect on C partitioning from slow to passive pools (t_7). On the other hand, the RMSE of the surrogate-based optimization and Bayesian MCMC are also similar, agreeing with the parameter calibration results.

Many calibrated parameters are very approximate to the assigned bounds (Fig. 8), suggesting that some assigned bounds are not so reasonable. The calibrated $c(12,12)$ value (1.01×10^{-3}) reaches its lower bound, indicating that passive SOC residence time almost reaches 1000 years. The calibrated temperature sensitivity (Q_{10}) decreases from 2 to 1.74 (Table 1). Soil microbial and passive pools increase due to longer residence time of passive pool and lower temperature sensitivity (Q_{10}). The size of the slow pool, on the contrary, decreases due to increase in exit rate from slow pool or decrease in its residence time. Comprehensively, the size of SOC, which is the sum of passive pool, slow pool and soil microbial pool, increase and more approximate to observation.

5.2 Analysis of Microbial Models

According to the calibrated RMSE and r^2 , the SOC simulation of the 2-pool and 4-pool microbial models are very similar. Therefore, we only analyse the parameter calibration results of the 4-pool microbial model. After parameter calibration using the surrogate-based optimization, the global SOC produced by the 4-pool microbial model are further improved, especially in China, Russia, Europe and North America (Fig. 9). Overall, the microbial model explains a higher fraction of global variability of the observed SOC data and had a lower spatial RMSE than the CLM-CASA' (Table 3).



Microbial models produce better SOC prediction than calibrated CLM-CASA' models in terms of C prediction in the low-temperature regions (Russia, Europe, North America) and in the regions with small soil C inputs (Fig. 7b and 9). The SOC contents are determined by two main factors, the soil carbon inputs and the SOC residence time (Luo et al., 2003). Considering the same soil carbon inputs of the CLM-CASA' and microbial models, the improvement is induced by the differences of SOC residence time. In CLM-CASA' and microbial models, the SOC residence time is both controlled partially by temperature (Xia et al. 2013). The difference is caused by the temperature sensitivities (Q_{10}), which is constant across space in the CLM-CASA'. Both two microbial models calculate spatially variable Q_{10} with higher values in the low-temperature regions and lower Q_{10} in the high-temperature regions, which is the influence of the temperature to the microbial activity. On the other hand, the SOC residence time is also influenced by quality of SOC inputs and related to microbial decomposition processes. Fresh C input stimulates microbial biomass growth, leading to the increase of old SOC decomposition rate (i.e., priming effect) (Kuzuyakov et al, 2000; Fontaine et al., 2004, 2007). Therefore, the microbial models simulate lower SOC residence times than the CLM-CASA' model in the areas with high SOC input and higher SOC residence times in the areas with low SOC input. This is because of the nonlinearity of substrate limitation in the microbial models (Equation 8 and 10), as well as the dependency of residence times on microbial biomass. Comprehensively, the introduction of microbial biomass helps microbial models predict SOC better than the CLM-CASA' model.

The posterior distribution of parameters calculated by Bayesian MCMC and the calibrated parameters by our surrogate-based optimization are presented in Fig. 10. According to the posterior distribution, r_d , CUE_{slope} , CUE_0 , E_a , par_{lig} and par_{clay} are most constrained and sensitive parameters. The calibration results of the surrogate-based optimization agree with the posterior distribution in these highly sensitive parameters (Fig. 10) except CUE_{slope} and CUE_0 . CUE_{slope} and CUE_0 are highly sensitive owing to their influence on temperature sensitivity. Due to the difference between CUE_{slope} and CUE_0 , the RMSE of the surrogate-based optimization is 1.4 kg/m^2 lower than Bayesian MCMC (Table 3).

6 Conclusions

Parameter calibration becomes more and more challenging for SOC model development. Bayesian MCMC approach has been used to typical SOC models while it's not applicable to computationally-expensive global land models owing to approximate one million simulations. In this study, we introduced the RBF surrogate-based optimization algorithm for the parameter calibration of computationally expensive SOC models. The main findings are:

- 1) The surrogate-based optimization based on RBF models gain more accurate calibration results than the Bayesian MCMC approach. The computation cost of the surrogate-based optimization is only 0.1% of the Bayesian MCMC.
- 2) Compared to advanced global optimization algorithms, the surrogate-based optimization is more effective and efficient on average. Our RBS surrogate-based optimization dominates other parameter calibration algorithms when the number of simulation is smaller than two hundred.



- 3) The surrogate-based optimization scheme is robust. Various types of surrogate models have the similar performance in parameter calibration tasks of SOC models.
- 4) Although the surrogate-based optimization is only guided by a single metric function value, it still can find the true parameter values. We carefully analyze the spatial SOC distributions produced by SOC models with the calibrated parameters of our surrogate-based optimization algorithm, indicating that the surrogate-based optimization truly improves the model prediction and simulation capability. The final calibrated parameter values of the surrogate-based model are also nearly the same as the Bayesian MCMC approach.

Nowadays, more and more complex simulation models present challenges to the surrogate-based optimization algorithm. To improve the accuracy of the surrogate-based optimization, better surrogate models are expected. Current surrogate models most employ only one surrogate model and we will focus on the application of multi surrogate models using ensemble learning.

7 Code and data availability

The code and data of three models and algorithms can be found in the supplement. If you have any problem when using the code, please feel free to contact the first author: Haoyu Xu (ocean920329@gmail.com).

References

- 15 Aleman D M, Romeijn H E, Dempsey J F. A response surface approach to beam orientation optimization in intensity-modulated radiation therapy treatment planning[J]. *INFORMS Journal on Computing*, 2009, 21(1): 62-76.
- Allison S D, Wallenstein M D, Bradford M A. Soil-carbon response to warming dependent on microbial physiology[J]. *Nature Geoscience*, 2010, 3(5): 336-340.
- Booker A J, Dennis Jr J E, Frank P D, et al. A rigorous framework for optimization of expensive functions by surrogates[J]. *Structural optimization*, 1999, 17(1): 1-13.
- 20 CHEN H, TIAN H Q. Does a General Temperature-Dependent Q10 Model of Soil Respiration Exist at Biome and Global Scale[J]. *Journal of Integrative Plant Biology*, 2005, 47(11): 1288-1302.
- Corzo G, Solomatine D. 2007 Special Issue: Knowledge-based modularization and global optimization of artificial neural network models in hydrological forecasting[J]. *Neural Networks the Official Journal of the International Neural Network Society*, 2007, 20(4):528-536.
- 25 Duan Q, Sorooshian S, Gupta V K. Optimal use of the SCE-UA global optimization method for calibrating watershed models[J]. *Journal of hydrology*, 1994, 158(3): 265-284.
- Duan Q, Sorooshian S, Gupta V. Effective and efficient global optimization for conceptual rainfall-runoff models[J]. *Water resources research*, 1992, 28(4): 1015-1031.



- Fontaine S, Bardoux G, Abbadie L, et al. Carbon input to soil may decrease soil carbon content[J]. *Ecology Letters*, 2004, 7(4):314-320.
- Fontaine S, Barot S, Barré P, et al. Stability of organic carbon in deep soil layers controlled by fresh carbon supply[J]. *Nature*, 2007, 450(7167):277-80.
- 5 Friedlingstein, P., et al. (2006), Climate-carbon cycle feedback analysis: Results from the C4MIP model intercomparison, *J. Clim.*, 19(14), 3337–3353, doi:10.1175/jcli3800.1.
- Friedman J H. Multivariate adaptive regression splines[J]. *The annals of statistics*, 1991: 1-67.
- German D P, Marcelo K R B, Stone M M, et al. The Michaelis–Menten kinetics of soil extracellular enzymes in response to temperature: a cross-latitudinal study[J]. *Global Change Biology*, 2012, 18(4): 1468-1479.
- 10 Giunta A A. Aircraft multidisciplinary design optimization using design of experiments theory and response surface modeling methods[D]. virginia polytechnic institute and state university, 1997.
- Global Soil Data Task Group (2000) Global Gridded Surfaces of Selected Soil Characteristics (IGBP-DIS). [Global Gridded Surfaces of Selected Soil Characteristics (International Geosphere-Biosphere Programme - Data and Information System)]. Data set, Oak Ridge National Laboratory Distributed Active Archive Center, Oak Ridge, TN.
- 15 Gutmann H M. A radial basis function method for global optimization[J]. *Journal of Global Optimization*, 2001, 19(3): 201-227.
- Haario H, Saksman E, Tamminen J. An adaptive Metropolis algorithm[J]. *Bernoulli*, 2001: 223-242.
- Hansen N, Kern S. Evaluating the CMA evolution strategy on multimodal test functions[C]//International Conference on Parallel Problem Solving from Nature. Springer Berlin Heidelberg, 2004: 282-291.
- 20 Hansen N, Ostermeier A. Completely derandomized self-adaptation in evolution strategies[J]. *Evolutionary computation*, 2001, 9(2): 159-195.
- Hansen N. Benchmarking the Nelder-Mead downhill simplex algorithm with many local restarts[C]//Proceedings of the 11th Annual Conference Companion on Genetic and Evolutionary Computation Conference: Late Breaking Papers. ACM, 2009: 2403-2408.
- 25 Hapuarachchi H A P, Li Z, Wang S. Application of SCE-UA method for calibrating the Xinanjiang watershed model[J]. *Journal of lake sciences*, 2001, 13(4): 304-314.
- Hararuk O, Smith M J, Luo Y. Microbial models with data-driven parameters predict stronger soil carbon responses to climate change[J]. *Global change biology*, 2015, 21(6): 2439-2453.
- Hararuk O, Xia J, Luo Y. Evaluation and improvement of a global land model against soil carbon data using a Bayesian Markov chain Monte Carlo method[J]. *Journal of Geophysical Research: Biogeosciences*, 2014, 119(3): 403-417.
- 30 Houghton, J. T., Y. Ding, D. J. Griggs, M. Noguier, P. J. van der Linden, X. Dai, K. Maskell, and C. Johnson (2001), *Climate Change 2001: The Scientific Basis*, Cambridge Univ. Press, Cambridge, doi:10.1002/qj.200212858119.



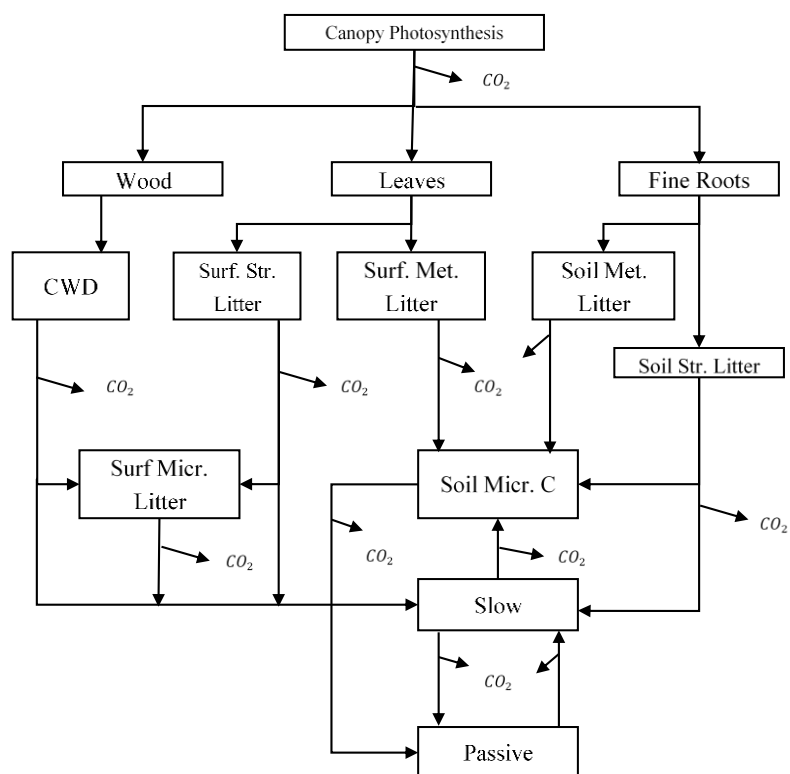
- Ise, T., and P. R. Moorcroft (2006), The global-scale temperature and moisture dependencies of soil organic carbon decomposition: An analysis using a mechanistic decomposition model, *Biogeochemistry*, 80(3), 217–231, doi:10.1007/s10533-006-9019-5.
- Jones D R, Schonlau M, Welch W J. Efficient global optimization of expensive black-box functions[J]. *Journal of Global optimization*, 1998, 13(4): 455-492.
- Jones, D.R. *Journal of Global Optimization* (2001) 21: 345. doi:10.1023/A:1012771025575
- Kennedy J. Particle swarm optimization[M]//Encyclopedia of machine learning. Springer US, 2011: 760-766.
- Kim K J. Toward Global Optimization of Case-Based Reasoning Systems for Financial Forecasting[J]. *Applied Intelligence*, 2004, 21(3):239-249.
- 10 Kuzuyakov Y, Friedel J K, Stahr K. Review of mechanisms and quantification of priming effects.[J]. *Soil Biology & Biochemistry*, 2000, 32(11–12):1485-1498.
- Li G, Cheng C, Lin J, et al. Short-term load forecasting using support vector machine with SCE-UA algorithm[C]//Third International Conference on Natural Computation (ICNC 2007). IEEE, 2007, 1: 290-294.
- Luo Y, A Ahlström, SD Allison, NH Batjes, V Brovkin, N Carvalhais, A Chappell, P Ciais, EA Davidson, A Finzi, K Georgiou, 15 B Guenet, O Hararuk, JW Harden, YJ He, F Hopkins, LF Jiang, C Koven, RB Jackson, CD Jones, MJ Lara, JY Liang, AD McGuire, W Parton, CH Peng, JT Randerson, A Salazar, CA Sierra, MJ Smith, HQ Tian, KEO Todd-Brown, M Torn, KJ van Groenigen, YP Wang, TO West, YX Wei, WR Wieder, JY Xia, X Xu, XF Xu, T Zhou. 2016. Towards More Realistic Projections of Soil Carbon Dynamics by Earth System Models. *Global Biogeochemical Cycles*, DOI: 10.1002/2015GB005239.
- Luo Y. Terrestrial carbon-cycle feedback to climate warming[J]. *Annual Review of Ecology, Evolution, and Systematics*, 2007: 20 683-712.
- Luo YQ, TF Keenan, M Smith, 2015. Predictability of the terrestrial carbon cycle. 2015. *Global Change Biology* 21, 1737-1751. DOI: 10.1111/gcb.12766
- Luo, Y., L. W. White, J. G. Canadell, E. H. DeLucia, D. S. Ellsworth, A. Finzi, J. Lichter, and W. H. Schlesinger (2003), Sustainability of terrestrial carbon sequestration: A case study in Duke Forest with inversion approach, *Global Biogeochem. Cycles*, 17(1), 1021, doi:10.1029/2002GB001923.
- 25 Luo, Y., L. Wu, J. A. Andrews, L. White, R. Matamala, K. V. R. Schäfer, and W. H. Schlesinger (2001), Elevated CO₂ differentiates ecosystem carbon processes: Deconvolution analysis of Duke Forest FACE data, *Ecol. Monogr.*, 71(3), 357–376, doi:10.1890/0012-9615(2001)071[0357: ecdecpl]2.0.co;2.
- MA H, DONG Z, ZHANG W, et al. Application of SCE-UA algorithm to optimization of TOPMODEL parameters [J][J]. 30 *Journal of Hohai University (Natural Sciences)*, 2006, 4: 001.
- Madescu G, Boldea I, Miller T J E. The optimal lamination approach (OLA) to induction machine design global optimization[C]// Ias Meeting, Ias '96. Conference Record of the. IEEE, 1996:574-580 vol.1.
- Maranas C D, Androulakis I P, Floudas C A, et al. Solving long-term financial planning problems via global optimization[J]. *Journal of Economic Dynamics & Control*, 1997, 21(8-9):1405-1425.



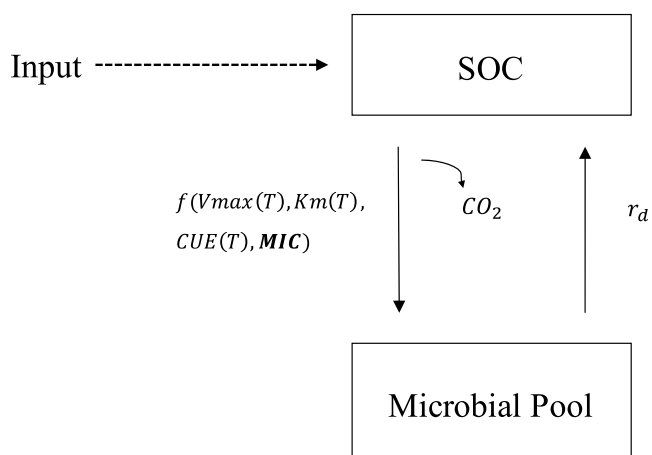
- Melillo, J. M., P. A. Steudler, J. D. Aber, K. Newkirk, H. Lux, F. P. Bowles, C. Catricala, A. Magill, T. Ahrens, and S. Morrisseau (2002), Soil warming and carbon-cycle feedbacks to the climate system, *Science*, 298(5601), 2173–2176, doi:10.1126/science.1074153.
- Müller J, Shoemaker C A. Influence of ensemble surrogate models and sampling strategy on the solution quality of algorithms for computationally expensive black-box global optimization problems[J]. *Journal of Global Optimization*, 2014, 60(2): 123-144.
- Myers R H, Montgomery D C, Anderson-Cook C M. Response surface methodology: process and product optimization using designed experiments[M]. John Wiley & Sons, 2016.
- Oleson, K. W., G. Niu, Z. Yang, D. Lawrence, P. Thornton, P. Lawrence, R. Stockli, R. Dickinson, G. Bonan, and S. Levis (2008), Improvements to the Community Land Model and their impact on the hydrological cycle, *J. Geophys. Res.*, 113, G01021, doi:10.1029/2007JG000563.
- Oleson, K. W., Y. Dai, G. Bonan, M. Bosilovich, R. Dickinson, P. Dirmeyer, F. Hoffman, P. Houser, S. Levis, and G.-Y. Niu (2004), Technical description of the community land model (CLM), NCAR Tech. Note NCAR/TN-461+ STR, 173.
- Parton, W. J., et al. (1993), Observations and modeling of biomass and soil organic matter dynamics for the grassland biome worldwide, *Global Biogeochem. Cycles*, 7(4), 785–809, doi:10.1029/93GB02042.
- Peng S, Piao S, Wang T, et al. Temperature sensitivity of soil respiration in different ecosystems in China[J]. *Soil Biology and Biochemistry*, 2009, 41(5): 1008-1014.
- Picheny V, Ginsbourger D, Richet Y, et al. Quantile-Based Optimization of Noisy Computer Experiments With Tunable Precision[J]. *Technometrics*, 2012, 55(1): 2-9.
- Price K, Storn R M, Lampinen J A. Differential evolution: a practical approach to global optimization[M]. Springer Science & Business Media, 2006.
- Regis R G, Shoemaker C A. A stochastic radial basis function method for the global optimization of expensive functions[J]. *INFORMS Journal on Computing*, 2007, 19(4): 497-509.
- Regis R G, Shoemaker C A. Parallel stochastic global optimization using radial basis functions[J]. *INFORMS Journal on Computing*, 2009, 21(3): 411-426.
- Regis R G. Stochastic radial basis function algorithms for large-scale optimization involving expensive black-box objective and constraint functions[J]. *Computers & Operations Research*, 2011, 38(5): 837-853.
- Schimel J P, Weintraub M N. The implications of exoenzyme activity on microbial carbon and nitrogen limitation in soil: a theoretical model[J]. *Soil Biology and Biochemistry*, 2003, 35(4): 549-563.
- Schonlau M, Welch W J, Jones D R. Global versus local search in constrained optimization of computer models[J]. *Lecture Notes-Monograph Series*, 1998: 11-25.
- Shi Y, Eberhart R C. Empirical study of particle swarm optimization[J]. *Frontiers of Computer Science in China*, 2009, 3(1):31-37.



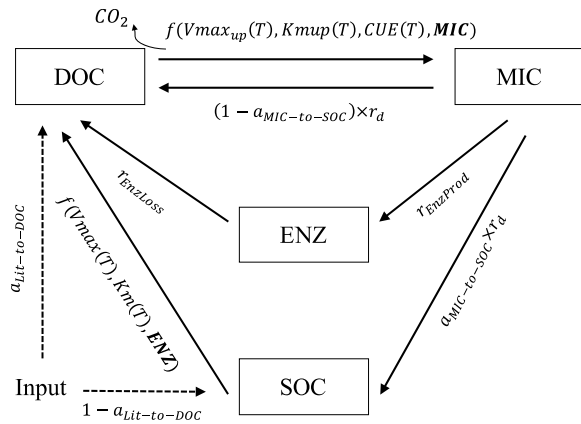
- Simpson T W, Mauery T M, Korte J J, et al. Kriging models for global approximation in simulation-based multidisciplinary design optimization[J]. *AIAA journal*, 2001, 39(12): 2233-2241.
- Smith, M. J., D. W. Purves, M. C. Vanderwel, V. Lyutsarev, and S. Emmott (2013), The climate dependence of the terrestrial carbon cycle, including parameter and structural uncertainties, *Biogeosciences*, 10(1), 583–606, doi:10.5194/bg-10-583-2013.
- 5 Sorooshian S, Duan Q, Gupta V K. Calibration of rainfall-runoff models: application of global optimization to the Sacramento soil moisture accounting model[J]. *Water resources research*, 1993, 29(4): 1185-1194.
- Storn R, Price K. Differential evolution—a simple and efficient heuristic for global optimization over continuous spaces[J]. *Journal of global optimization*, 1997, 11(4): 341-359.
- Taylor, K. E., R. J. Stouffer, and G. A. Meehl (2011), An overview of CMIP5 and the experiment design, *Bull. Am. Meteorol.*
- 10 *Soc.*, 93(4), 485–498, doi:10.1175/BAMS-D-11-00094.1.
- Todd-Brown, K. E. O., J. T. Randerson, W. M. Post, F. M. Hoffman, C. Tarnocai, E. A. G. Schuur, and S. D. Allison (2013), Causes of variation in soil carbon simulations from CMIP5 Earth system models and comparison with observations, *Biogeosciences*, 10(3), 1717–1736, doi:10.5194/bg-10-1717-2013.
- Wang C, Duan Q, Gong W, et al. An evaluation of adaptive surrogate modeling based optimization with two benchmark
- 15 problems[J]. *Environmental Modelling & Software*, 2014, 60(76):167-179.
- Weng, E., and Y. Luo (2011), Relative information contributions of model vs. data to short- and long-term forecasts of forest carbon dynamics, *Ecol. Appl.*, 21(5), 1490–1505, doi:10.1890/09-1394.1.
- Wieder W R, Bonan G B, Allison S D. Global soil carbon projections are improved by modelling microbial processes[J]. *Nature Climate Change*, 2013, 3(10): 909-912.
- 20 Xia, J., Y. Luo, Y. P. Wang, and O. Hararuk (2013), Traceable components of terrestrial carbon storage capacity in biogeochemical models, *Global Change Biol.*, 19, 2104–2116, doi:10.1111/gcb.12172.
- Xia, J., Y. Luo, Y. Wang, E. Weng, and O. Hararuk (2012), A semi-analytical solution to accelerate spin-up of a coupled carbon and nitrogen land model to steady state, *Geosci. Model Dev.*, 5(5), 1259–1271, doi:10.5194/gmd-5-1259-2012.
- Xu, T., L. White, D. Hui, and Y. Luo (2006), Probabilistic inversion of a terrestrial ecosystem model: Analysis of uncertainty
- 25 in parameter estimation and model prediction, *Global Biogeochem. Cycles*, 20, GB2007, doi:10.1029/2005GB002468.
- Zhou, T., P. Shi, D. Hui, and Y. Luo (2009), Global pattern of temperature sensitivity of soil heterotrophic respiration (Q₁₀) and its implications for carbon-climate feedback, *J. Geophys. Res.*, 114, G02016, doi:10.1029/2008JG000850.



(a) The CLM-CASA' model



(b) 2-pool microbial model



(c) 4-pool microbial model

Figure 1. Schematic representation of (a) CLM-CASA model, (b) 2-pool microbial model and (c) 4-pool microbial models

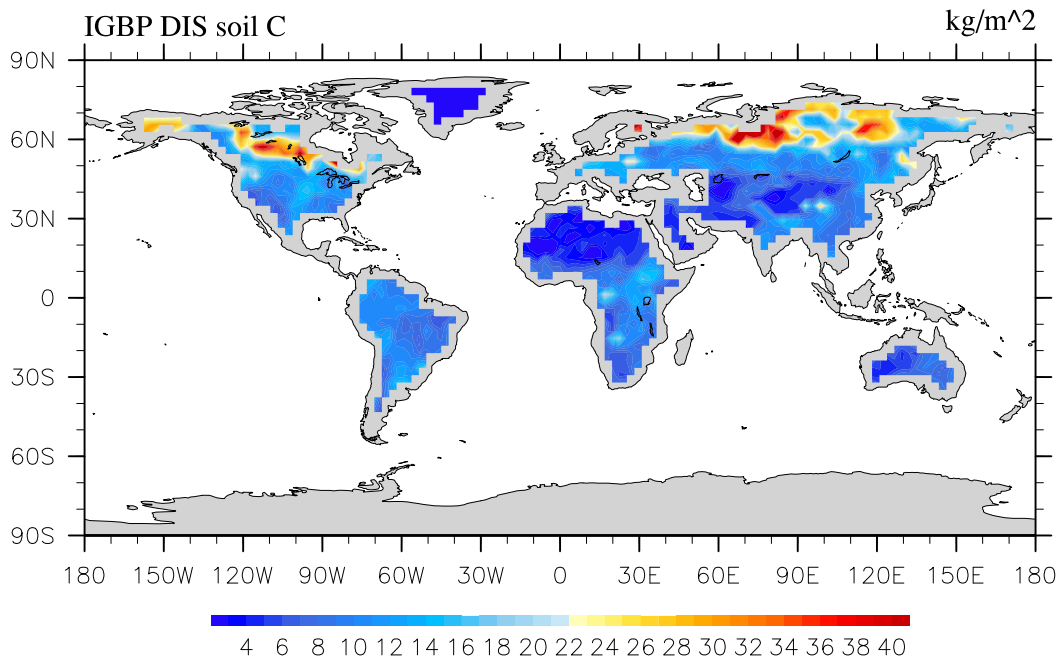


Figure 2. IGBP-DIS soil carbon distribution. Soil carbon varies from $0 kg/m^2$ in deserts to $60 kg/m^2$ in boreal regions

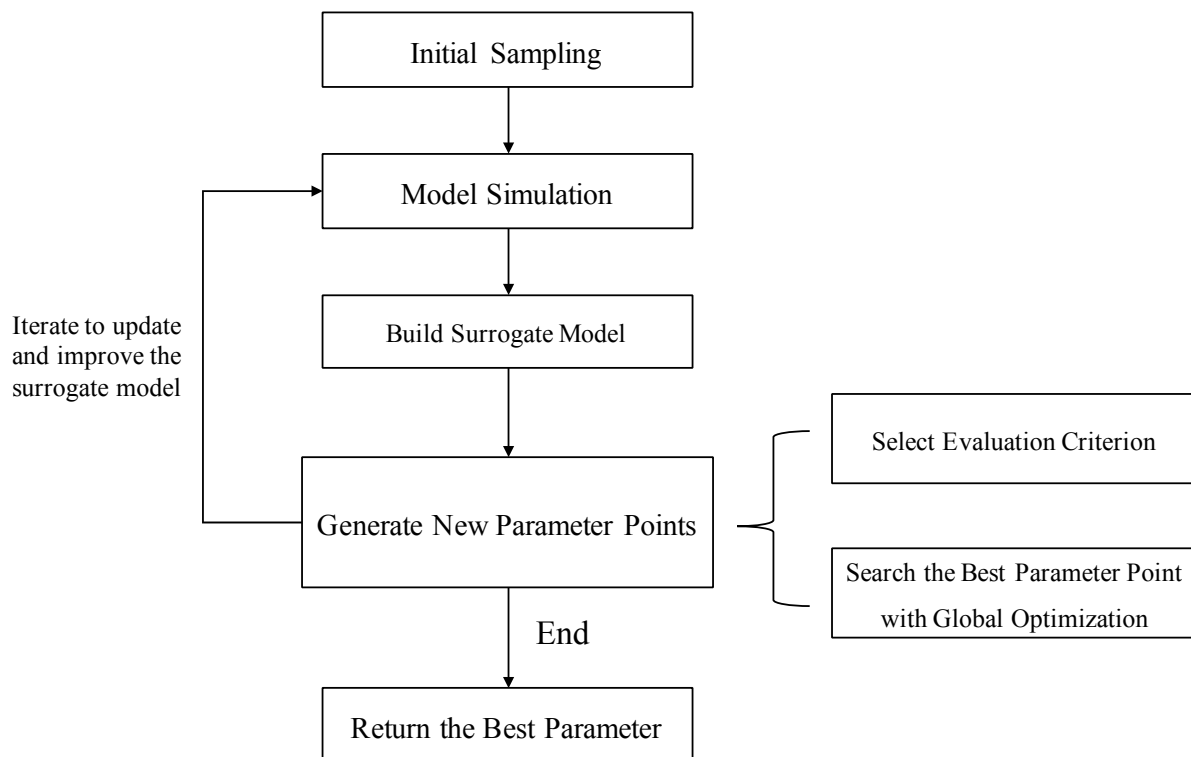
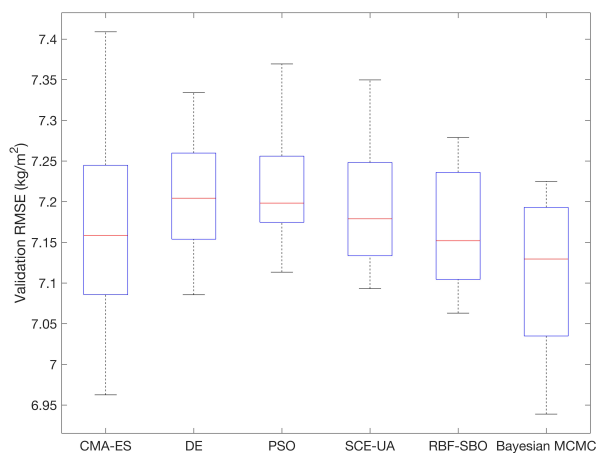
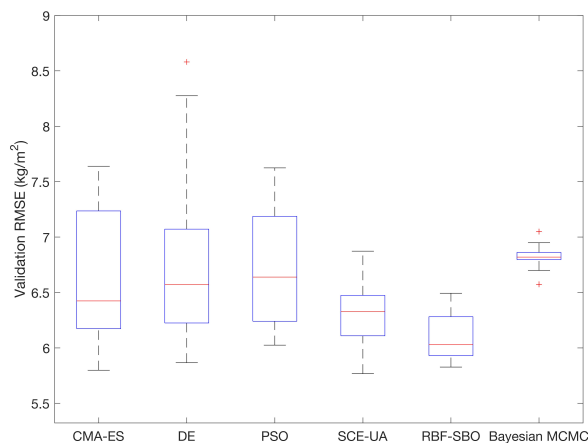


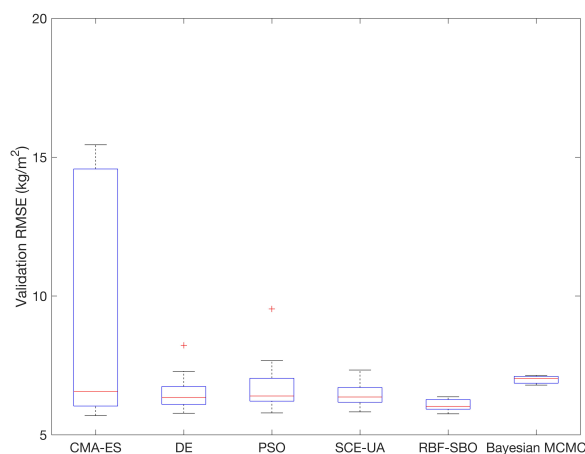
Figure 3. The scheme of the surrogate-based optimization



(a) CLM-CASA' model

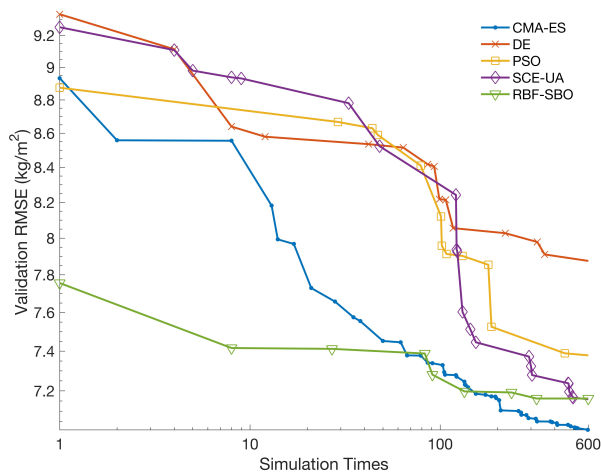


(b) 2-pool microbial model

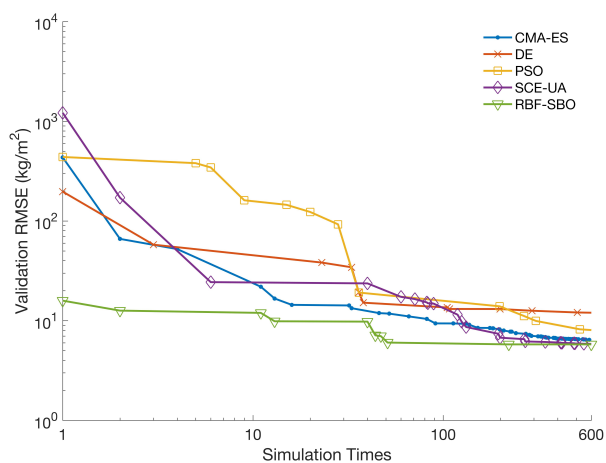


(c) 4-pool microbial model

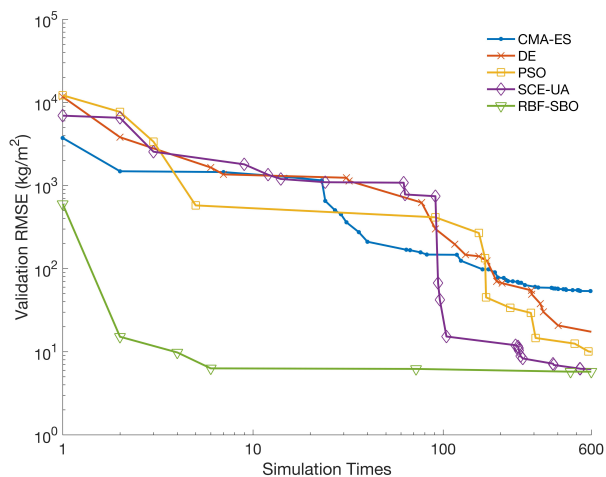
Figure 4. The final validation RMSEs of different parameter calibration algorithms: (a) CLM-CASA' model; (b) 2-pool microbial model and (c) 4-pool microbial model. The center line indicates the median; the bottom and top of the box are the first and third quartiles; the black bottom and top lines out of the rectangles are the maximum and minimum; the red crosses represent the exceptions. The simulation times of former 5 algorithms are 100 and the simulation times of Bayesian MCMC are presented in Table 3.



(a) CLM-CASA' model

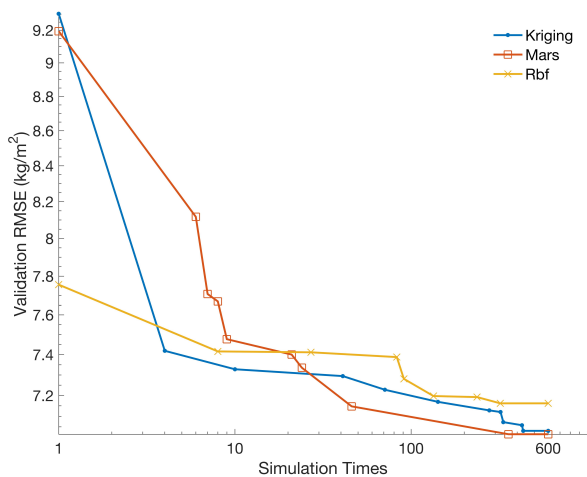


(b) 2-pool microbial model

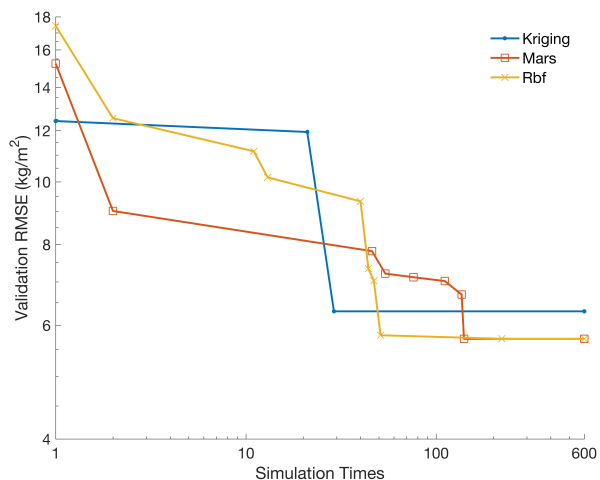


(c) 4-pool microbial model

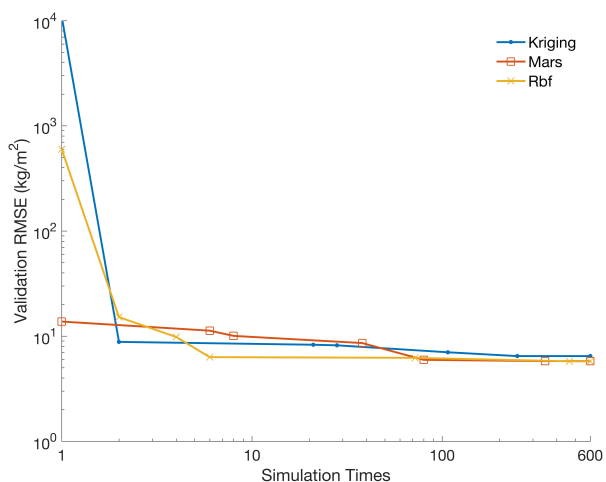
Figure 5. The average validation RMSE of the different algorithms as a function of the simulation times: (a) the CLM-CASA' model; (b) 2-pool microbial model and (c) 4-pool microbial model.



(a) CLM-CASA' model



(b) 2-pool microbial model



(c) 4-pool microbial model

Figure 6. The average validation RMSE among Kriging, Mars and RBF surrogate models.

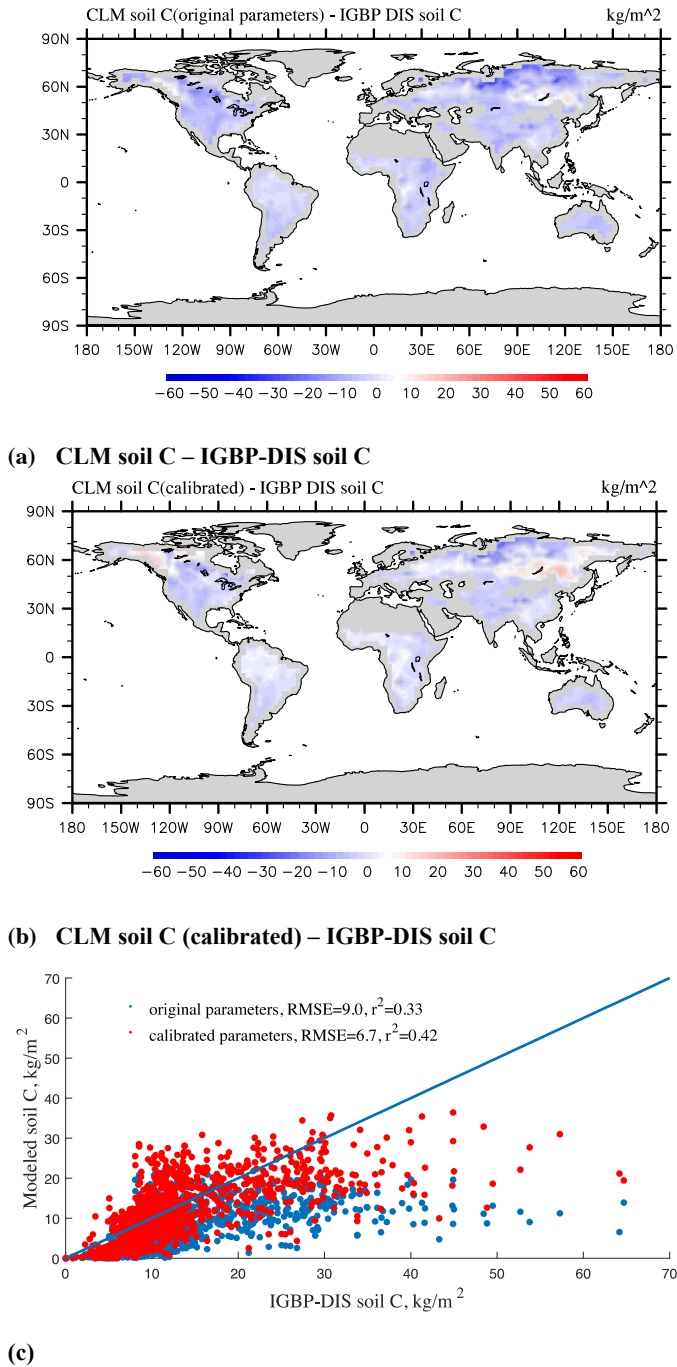


Figure 7. Spatial correspondence of CLM-CASA’ produced SOC to the IGBP-DIS reported SOC (a, c) before and (b, c) after parameter calibration using optimization technique. The points in Fig. 7c represent the grid cell values. CLM-CASA’ with the default parameters explains 33% of variation in the observed soil C, while CLM-CASA’ with the calibrated parameters explains 41% of variability in the observed soil C.

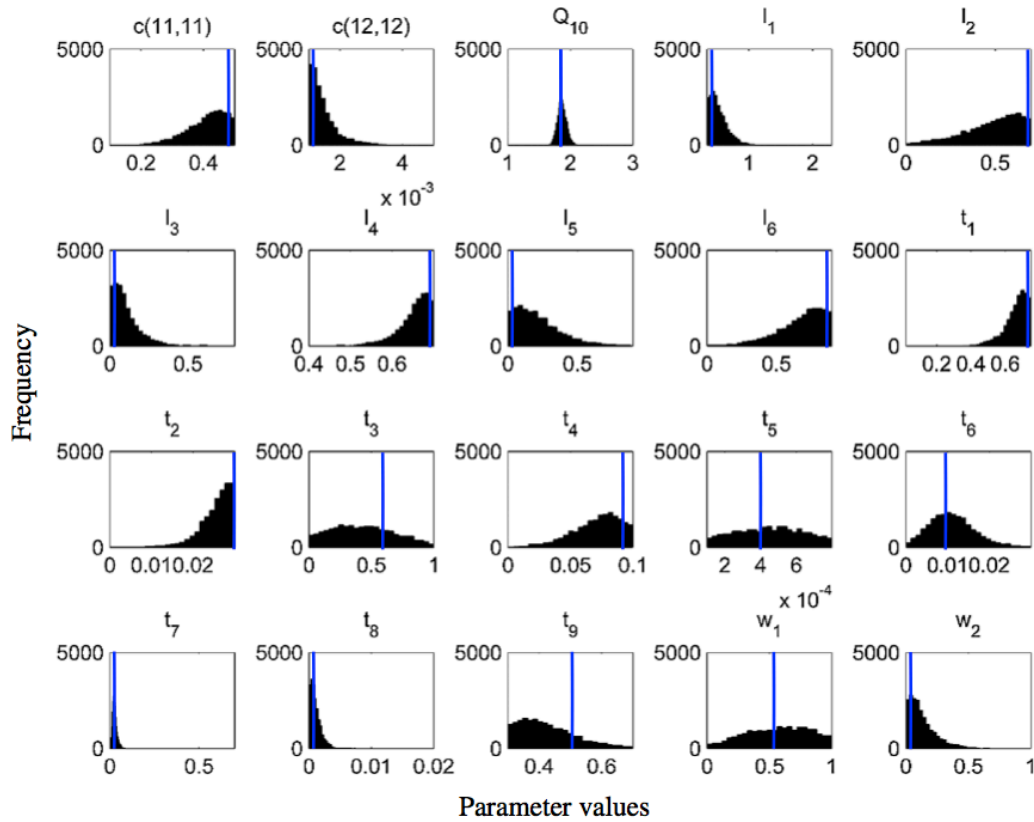


Figure 8. Frequency distributions of 20 calibrated parameters of CLM-CASA' model by Bayesian MCMC approach (Harauk, 2014) and surrogate-based optimization (blue line in each sub plot).

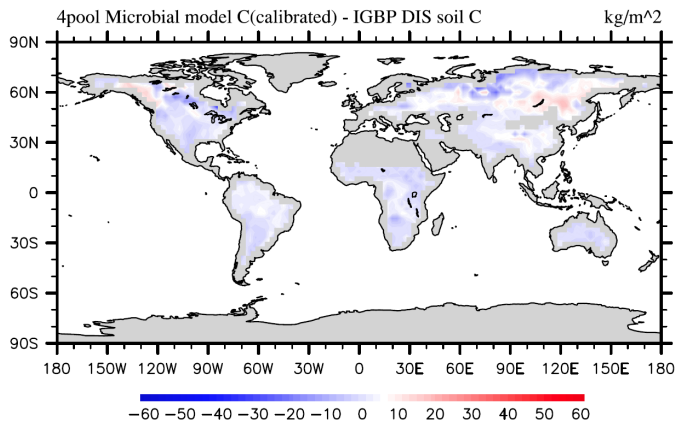


Figure 9. Spatial correspondence of 4-pool microbial model produced SOC to the IGBP-DIS reported SOC.

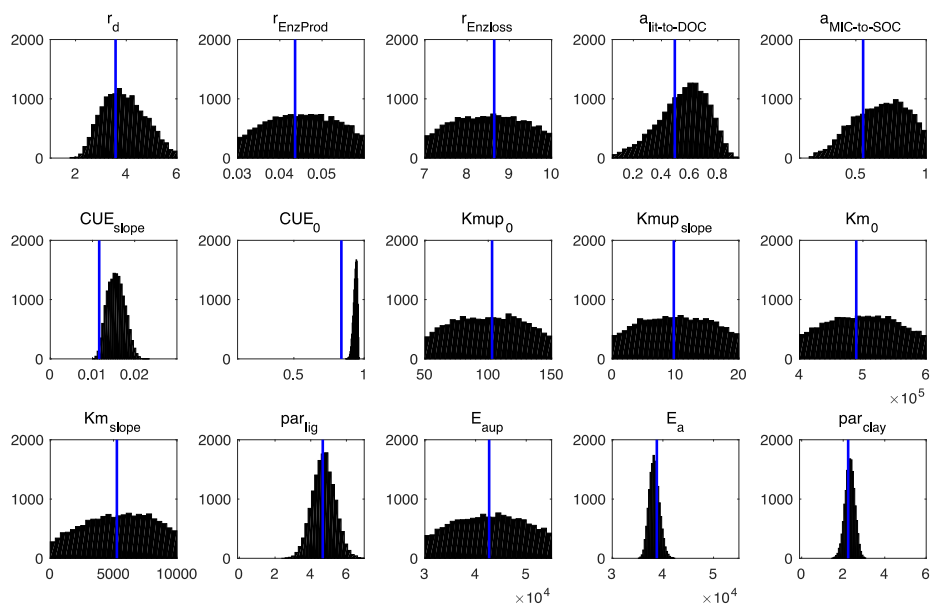


Figure 10. Posterior probability density functions of the 4-pool microbial model parameters (generated by Bayesian MCMC). The blue vertical lines are the final calibrated parameters by our surrogate-based optimization.



Table 1. Parameter description of CLM-CASA' C-only model

Parameter Description	Symbol	Default Value $\times 10^{-3}$	Calibrated Value by SBO $\times 10^{-3}$
Exit rate from slow pool	$c(11,11)$	200	495.6
Exit rate from passive pool	$c(12,12)$	4.5	1.01
Temperature sensitivity of C decomposition	Q_{10}	2000	1737
Labile C fraction effect on C partitioning from leaves to surface metabolic litter	w_1	1000	589.04
Labile C fraction effect on C partitioning from roots to soil metabolic litter	w_2	200	4.52
Partitioning from surface structural to surface microbial pool if no lignin in surface structural litter	l_1	400	384.5
Lignin effect of partitioning from surface structural litter to surface microbial litter	l_2	400	689
Lignin effect on partitioning from surface structural litter to soil slow pool	l_3	700	7.499
Partitioning from soil structural to soil microbial pool if no lignin in soil structural litter	l_4	450	697.7
Lignin effect on partitioning from soil structural litter to soil microbial pool	l_5	450	54.46
Lignin effect on partitioning from soil structural litter to soil slow pool	l_6	700	871.5
C partitioning from soil microbial pool to slow pool if no sand or clay	t_1	169	747.7
Clay effect on C partitioning from soil microbial pool	t_2	5.44	29.6
Sand effect on C partitioning from soil microbial to slow pool	t_3	678	636.8
Combined effect of sand and clay on C partitioning from soil microbial pool	t_4	22	99.5
C partitioning from soil microbial to passive pool if no sand or clay	t_5	0.51	0.152
Sand effect on C partitioning from soil microbial to passive pool	t_6	2.04	12.99
Clay effect on C partitioning from slow pool to passive pool	t_7	4.05	24.2
C partitioning from slow to passive pool if no clay	t_8	14	0.012
C partitioning from slow to soil microbial pool if no clay	t_9	449	368.8



Table 2. Parameter and description of the 4-pool microbial models

Parameter Name	Parameter Description	Default Value	Calibrated Value by SBO
r_d	Microbial death rate	4.38	4.89
CUE_0	Baseline microbial carbon use efficiency	0.63	0.965
CUE_{slope}	CUE_0 dependency on temperature	0.016	0.00853
Km_0	Baseline half saturation constant	500000	498467
Km_{slope}	Km_0 dependency on temperature	5000	9751
E_a	Activation energy of SOC decomposition	47000	36669
par_{clay}	Clay limitation	0	2.41
par_{lig}	Lignin-dependent correction factor	0	6.23
$r_{EnzProd}$	Rate of enzyme production	0.0438	0.0361
$r_{EnzLoss}$	Rate of enzyme loss	8.76	8.08
$a_{lit-to-DOC}$	Fraction of $Input_{soil}$ that is transferred to soil	0.3	0.832
$a_{MIC-to-SOC}$	Fraction of dead microbes transferred to soil	0.5	0.716
$Kmup_0$	Baseline half-saturation constants for substrate limitation of DOC uptake	100	134
$Kmup_{slope}$	$Kmup_0$ dependency on temperature	10	4.62
E_{aup}	Activation energy of DOC uptake	47000	34811

Table 3 Calibration results of Bayesian MCMC and our surrogate-based optimization

SOC model	Detail	Method	Lowest RMSE ($kg \cdot m^{-2}$)	Variance Explained	Number of Simulations
2-pool microbial	8 parameters	Bayesian MCMC	6.609	51.6%	50,000+500,000
	2 carbon pools	RBF-SBO	5.785	51.6%	221
4-pool microbial	15 parameters	Bayesian MCMC	7.142	51.3%	50,000+500,000
	4 carbon pools	RBF-SBO	5.756	51.4%	199
CLM-CASA'	20 parameters	Bayesian MCMC	7.000	41.0%	50,000+1,000,000
	13 carbon pools	RBF-SBO	7.162	42.8%	321